Invited Paper

THz Electron Spin Resonance on Nanomagnets

Hiroyuki Nojiri [1*, 2], Z. W. Ouyang [2]

[1] Institute for Materials Research, Tohoku University, Sendai 980-8577, Japan
[2] Wuhan National High Magnetic Field Center, HUST, Wuhan, 430074, China.

[*1] E-mail: nojiri@imr.tohoku.ac.jp

Abstract: Recent results of THz Electron Spin Resonance (ESR) on nanomagnets were reviewed. This article addresses (1) investigation of exchange coupling in heterometallic nanomagnets and chemical trends, (2) spin freezing in a giant nanomagnet, where quasi-spin wave like excitation is found without a phase transition in thermodynamic limit, and (3) pulsed EPR on a spin coherent experiment. Recent development of a tabletop THz spectrometer using a mini-pulsed magnet is also described. The development of a high-frequency ESR station at the Wuhan National High Magnetic Field Center at HUST is also introduced briefly. This article demonstrates the power of THz ESR for investigations of nanomagnets.

1. Introduction

Nanomagnets have attracted much attention for their distinct quantum dynamics, diversity of magnetism and possible application for information science. The important energy scales of nanomagnets such as anisotropy energy and exchange coupling are often in the THz regime. Thus, THz spectroscopy is an important tool for use in examining nanomagnets.

Compared with other techniques such as optical spectroscopy and neutron scattering, ESR presents advantages of high energy-resolution, clear magnetic selection rules, and sensitivity. In conventional spectroscopy, strong absorption arises from the electric–dipolar transition and not by magnetic–dipolar transition. Therefore, the spectrum is not sensitive to quantum numbers of nanomagnets such as spin S and its z-component S_z. However, extreme sensitivity such as a single photon counting is possible with spectroscopy. The disadvantage of neutron scattering determining the magnetic levels is in low sensitivity. A sample of a few grams is needed in many cases, which limits the application of neutron scattering for nanomagnets. The advantage of neutron scattering for spectroscopy and ESR is in its capability of measuring the correlation function that originates from the wave-vector dependence of the scattering.

The selection rule of ESR is known as $\Delta S_z = \pm 1$ and $\Delta S = 0$. In fact, intra-multiplet transitions can be observed in most cases. Inter-multiplet transitions such as the singlet-triplet transition of $\Delta S = \pm 1$ can also be observed if mixing among different magnetic quantum states exists as a result of certain types of anisotropies and interactions such as Dzyaloshinskii–Moriya term and staggered field. These terms change the mixing between the states with different total S. In rare-earth ions, the magnetic states are marked by total J and not by total S because of the

unquenched orbital moment. In this case, the ESR spectrum is greatly complicated because the total J is not a good quantum number for the complicated crystal field splitting of rare-earth ions in a low-symmetry environment around the ions.

ESR has been developed in the microwave regime. Even now most conventional systems are used at the so-called X-band of 9.5 *GHz*. The frequency is related to the magnetic field of 0.3 *T*. Higher frequencies are available in a customized spectrometer in sub-THz regime. Such a system needs a high magnetic field to cover the large Zeeman energy. For example, 400 *GHz* is related to the resonance field of 14.3 *T* for free electron spins. Consequently, a superconducting magnet is used in most sub-THz spectrometers. Another way is to use a pulsed magnet, which can generate a high magnetic field above 30 *T*. In fact, ESR of free electron spins at 1 *THz* is related to the magnetic field of 35.7 *T*. The combination of THz source and a pulsed magnet is unique to cover the wide energy and the magnetic field range of a THz ESR spectrometer.

A pulsed magnetic field generator has been regarded as large equipment. However, miniaturization of the system has been proposed with the concept of a "portable pulse magnet" and is realized in combination with X-ray and neutron beam experiments. The use of a "portable magnet" is now extended for the THz spectroscopy. It enables us to use a tabletop magnetic field generator of 30 *T* for time-resolved THz spectroscopy.

In the following, we describe the ESR system at IMR and at HUST as examples of THz-ESR spectrometers. Then examples for applications on nanomagnets are reviewed. Finally, the possibility of table top THz spectroscopy using a portable pulsed magnet will be introduced.

2. Experimental Setup

2.1. THz ESR spectrometer at IMR
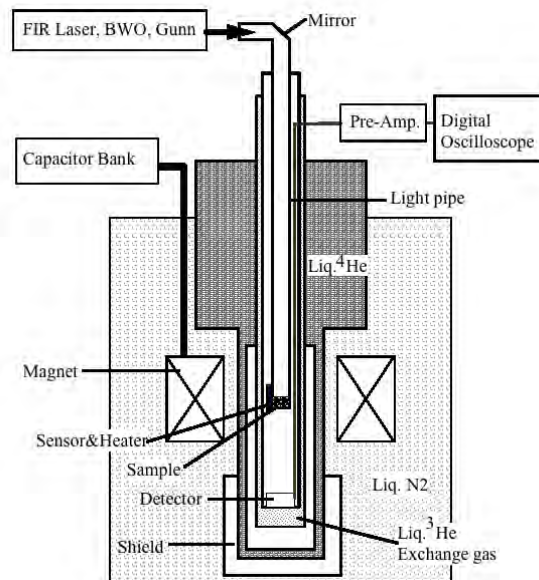
Fig. 1 Schematic view of the TESRA-IMR. The setup with ^{3}He insert is shown.

Fig. 1 shows a schematic view of the Terahertz Electron Spin Resonance Apparatus (TESRA-IMR) installed at the magnetism division of Institute of Materials Research (IMR), Tohoku University. Details of the system were described in an earlier report [1]. The major components of the system are a capacitor bank, cryostats, detectors, and light sources. The capacitor bank energy is 90 *kJ* with the 7.2 *mF*, 5 *kV* capacitor. A typical rise time is 2.5 *ms* and the full pulse width is stretched to 25 *ms* using a crowbar circuit. 40 *T* and 30 *T* can be generated respectively in 16-*mm*-diameter and 21-*mm*-diameter solenoid magnets. A gas-flow type cryostat and a conventional ^{4}He bath type cryostat with ^{3}He insert options are used. The loading of a sample can be made by a top-loading mechanism for quick replacement.

As the radiation source, we use Gunn oscillators with multiplier options. An optical pumped far-infrared laser is used for higher frequency. Backward travelling wave oscillators (BWO) are also used in limited frequency bands such as 35-190 *GHz* and 350-400 *GHz*.

The ESR spectrum is taken by sweeping a magnetic field at a fixed frequency. No modulation of the magnetic field or of the radiation source is used. The detector is AC-coupled. Therefore, shifting of the signal caused by the change of sample absorption under the pulsed magnetic field sweep is detected as the time dependence of the signal. It is subsequently converted to the magnetic field dependence of the transmission. The transient waveform is captured using a digital oscilloscope. It is then processed using the software.

2.2. High magnetic field ESR system at HUST

Figure 2 presents an outline of High-field high-frequency ESR facility recently developed at the Wuhan National High Magnetic Field Center, HUST. The system consists of gas-flow type cryostat, pulsed magnet, ESR probe, light source, and data-acquisition system arranged in a Faraday box. With the ^{4}He cryostat, a sample temperature of 2.0 *K* can be achieved. Magnetic fields up to 40 *T* can be generated using a pulsed magnet driven by a 0.8 *MJ* capacitor bank. As the light source, a BWO, which can generate electromagnetic waves of 210-370 *GHz*, was installed. The coverage of frequency and the magnetic field are unique in China [2]. The ESR spectrum is collected by sweeping a magnetic field at fixed frequency. In the second stage of the ESR project, the frequency coverage will be extended between 60 and 500 *GHz* using both Gunn oscillators and BWOs.
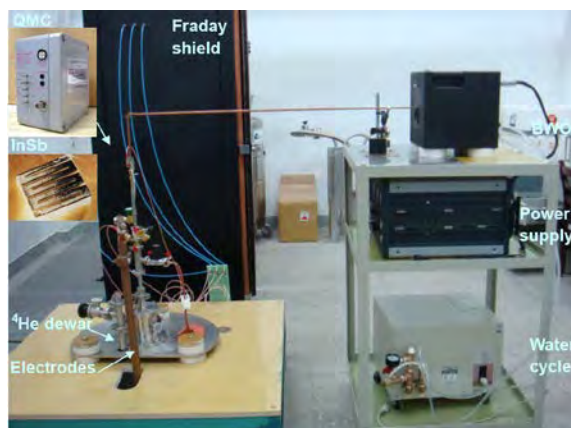
Fig. 2 Outline of the high-field ESR facility at HUST.

3. Determination of exchange coupling of hetero-metallic nanomagnet

Tremendous efforts have been undertaken in synthesizing exchange-coupled high spin nanomagnets made up of 3d transition metal ions. The most well known example is Mn_{12} with an S=10 ground state. The exchange coupling of a 3d metal ions based system is sizable to stabilize the high spin ground states. However, the anisotropy necessary to stabilize the directions of the moments is not very strong in 3d transition metal ions because of the quenching of the orbital moments and of the moderate spin–orbit coupling. An alternative candidate is rare-earth ions with large moments and strong anisotropies. However, rare-earth-based nanomagnets have a fundamental limitation for weak exchange coupling. To break through this limit, efforts have been made to synthesize a heterometallic system combining 3d transition metal and rare-earth ions. More recently, a combination of the radical and the rare-earth ions has also been developed. The latter has greater diversity in structure for the flexible design of the organic framework.

To push the cycle of material development, the accurate, systematic, and easy evaluation of the exchange coupling is necessary. A most conventional mode of estimate is the fitting of the temperature dependence of the magnetic susceptibility. However, the complicated splitting of the rare-earth ions makes the fitting extremely difficult. In other words, the unique set of exchange parameter cannot be obtained using this method. Moreover, calculation of the energy levels of the rare-earth ions is extremely time-consuming for a large Hilbert space. To determine the total view of the energy level, neutron scattering is ideal. The request for the large sample amount and the limited facility access make this method difficult for wide applications.

(a)   (b)
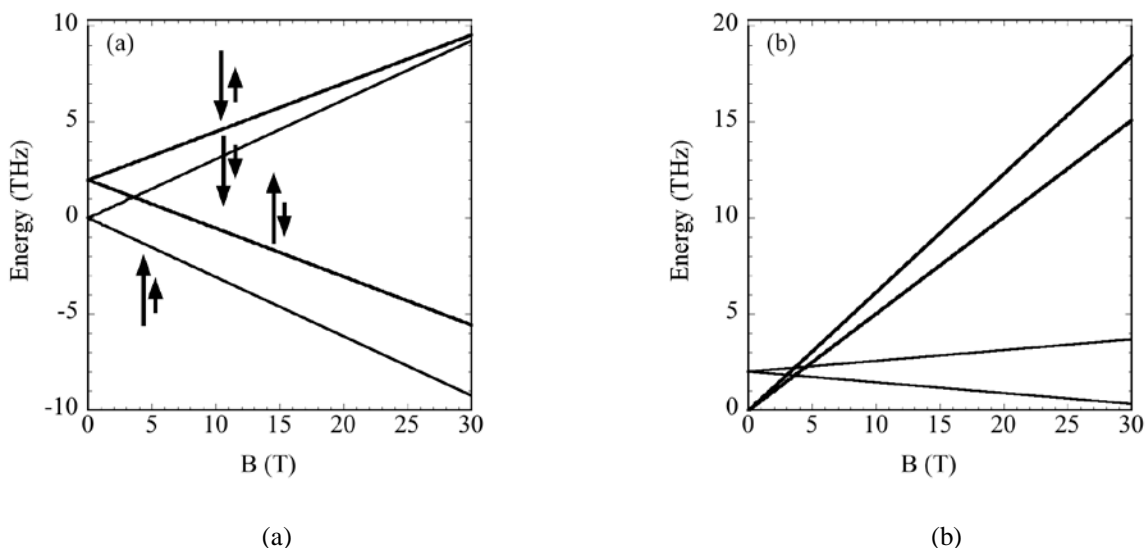
Fig. 3(a) Schematic energy diagram of the heterometallic system. Large and the short arrows respectively represent rare-earth and 3d transition metal magnetic moments. (b) Schematic frequency-field diagram. Thin lines and thick lines originate, respectively, from the flip of the 3d transition metal and rare-earth magnetic moments.

For determining the exchange coupling of a heterometallic system THz ESR can be a uniquely useful tool [3-7]. Fig. 3(a) portrays a schematic energy diagram of the low energy levels of such a system. The large and the short arrows respectively represent the total angular momentum of a rare-earth ion J_r and a 3d transition metal spin of S=1/2 (Cu^{2+} or V^{4+}). In the energy level diagram,

only one doublet of the rare-earth moment is included. For free ions, this doublet must be the one with the largest z-component of J_r. Other excited states of rare-earth ions are neglected in the present diagram. Such simplification can be justified if the system is investigated only at low temperature. The experiment of THz ESR meets such conditions because the spectrum must be dominated by the transitions in the low energy states at low temperatures.

Fig. 3(b) presents the possible frequency-field diagram of such system. The modes with smaller slope originate by the flip of the $S=1/2$ spin. Steep modes are caused by the flip of the rare-earth moment. One can regard the former mode as the ESR of $S=1/2$ spin with exchange bias, where the resonance field shifts for the exchange field. However, from an alternative perspective, the transition is as unconventional as ESR because the total angular momentum changes in such a transition. More explicitly, the total J_t of the heterometallic system changes, where the J_t is given as the coupling of J_r and S. It apparently breaks the selection rule of ESR formulated as $\Delta J_z = \pm 1$ and $\Delta J = 0$. Here S is replaced by the total angular momentum. At this stage, it is noteworthy that the selection rule is valid only when $\square J_z$ and J are good quantum numbers. It means that a forbidden and unconventional EPR are visible by mixing of the different magnetic levels. In rare-earth ions, such mixing often happens when the ion is located in the crystal.

Fig. 4 portrays an example of an ESR spectrum showing the several modes of transition [3]. The main strong transitions are assigned as the flip of the spin of the 3d transition ions from the slope of the modes. Weak modes are regarded as those caused by the flip of rare-earth ions. In fact, the slopes are steep for the large change of the total angular momentum. Observation of those modes indicates the existence of the mixing caused by the crystal field splitting of rare-earth ions. The proof of this interpretation is given by the missing of such unconventional ESR when the rare-earth ion is Gd. In case of Gd, the angular momentum is absent. Therefore, the ESR selection rule is kept without modification.
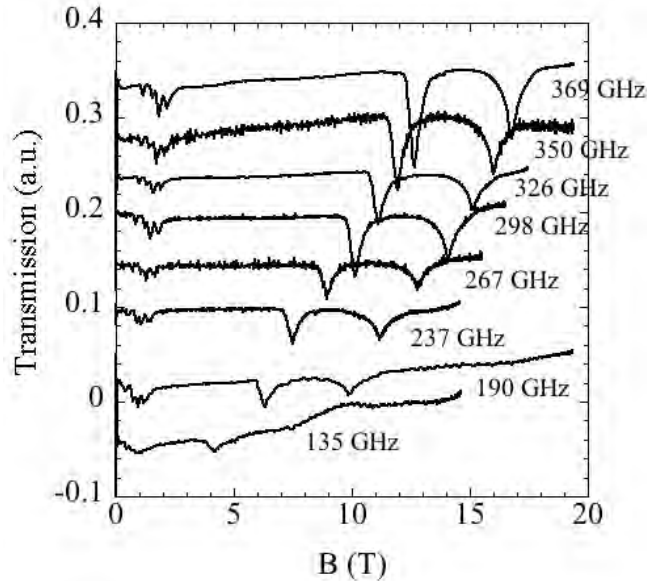
Fig. 4 ESR spectrum of DyV heterometallic nanomagnet.

4. Spin freezing in a giant nanomagnet

Recently, high symmetrical molecular clusters called spin polyhedra have been investigated. The most well known family is designated as "Keplarate", which are homo-metallic clusters with icosidodecahedral shape. Spins are sitting on the 30 corners of the network made up of 20 triangles and 10 pentagons. As the magnetic ions, half-integer series including $S=1/2$ V^{4+}, $S=3/2$ Cr^{3+}, and $S=5/2$ Fe^{3+} have been examined and antiferromagnetic coupling between the spins is found in all of those.

A singlet ground state is expected if an isotropic Heisenberg model can describe a cluster. In fact, $S=1/2$ system has the singlet ground state with sizable single-triplet excitation gap [8]. For $S=3/2$ Cr^{3+} and $S=5/2$ Fe^{3+}, slowing of the spin motion is expected toward zero temperature [9]. In the bulk system with large site spin and next-neighbor antiferromagnetic interaction, the most conventional ground state is an antiferromagnetic ordered state because of the lack of singlet ground state formation in $S=3/2$ and $S=5/2$ site spins associated only with small quantum fluctuations. A spin glass state might take place in a system with disorder. The interest is in the characteristics of the ground state of finite, but with large clusters with large site spin-like Keplarate. Such a system is not a bulk system. However, the states are very numerous because of the 30 spin sites.

Fig. 5 shows the temperature-dependence of the ESR spectrum for the $S=5/2$ cluster. The temperature dependence of the line width and the resonance field are depicted in Fig. 6, where a distinct anomaly is found. The line width increases rapidly with decreasing temperature and takes a maximum at around 2–2.5 K. A decrease of the width is found below the peak temperature. Such behavior is similar to the temperature dependence of ESR line width at magnetic ordering. Namely, the line width increases for the short-range spin correlation near the ordering temperature. The width decreases below the ordering temperature for suppression of fluctuation by the magnetic order. We measured specific heat, which is the probe at thermodynamic limit. Distinct peaks are apparent and the temperature is identical to the anomaly temperature found by ESR.
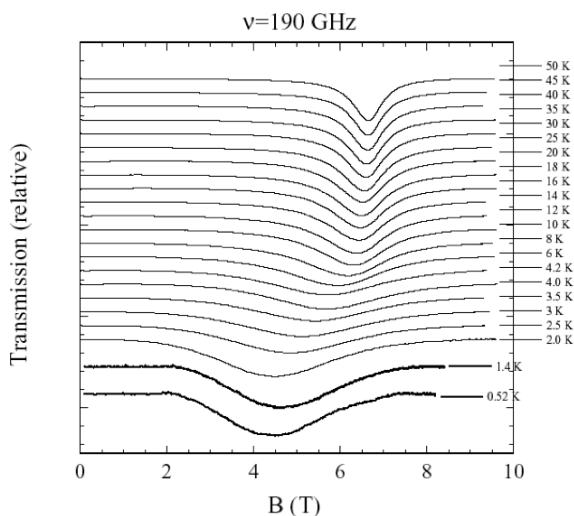
Fig. 5 Temperature dependence of ESR spectrum of Fe_{30} cluster at 190 GHz. The sample is polycrystalline.
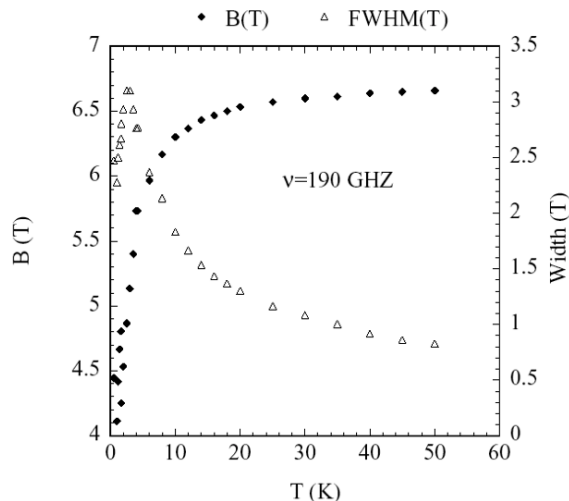
Fig. 6 Temperature dependence of line width (right-axis) and the resonance field (left-axis) at 190 *GHz*. The line width shows a peak around 2.5 *K*. The resonance field shows a large shift below 10 *K*.

We speculate that a quasi-ordering or spin freezing takes places in the system. Namely, a critical slowing toward the zero temperature is quenched at finite temperature and a major part of entropy is lost. However, the real magnetic order does not occur because the system is finite and the correlation function cannot divert to infinite. Below the quasi-ordering temperature, a spin-wave-like mode might arise. In fact, we found an antiferromagnetic-resonance-like mode with a finite excitation gap. ESR is useful to investigate those behaviors because it is sensitive to the short-range correlation. ESR is also unique to capture the corrective motion such as spin wave because of the long wavelength and q=0 excitation nature. Theoretical considerations are also made on this point [10-12].

5. Pulsed EPR for spin coherent manipulation

Pulsed spin echo EPR is a powerful and unique tool for spin manipulation based on quantum mechanics. S=1/2 state of nanomagnet can be regarded as a basic unit of quantum Q-bit. The first step of realization of Q-bit is the observation of time evolution of probabilities of spin–up and spin–down states called Rabi oscillation. The two major difficulties of finding Rabi oscillation are the spin–lattice relaxation and spin–spin relaxation. The former process can be suppressed by operation at low temperatures. However, spin–spin relaxation is difficult to remove completely because the main cause is the magnetic dipolar interaction. This interaction exists in any magnetic system. The coupling is sizable among distant neighbors [13-18].

Several investigations have been made for Rabi-oscillation on nanomagnets. Most have been made in diluted frozen solution form to reduce the intermolecular coupling. Such dilution reduces the uniqueness of using nanomagnets. In fact, the observation of Rabi oscillation is much simpler in the isolated single spin such as impurity in non-magnetic crystal, defect and color center. It is necessary to develop a new system that can accommodate scalable operation.

Recently, a Rabi oscillation experiment was done using a triangular nanomagnet: {Cu_3} adsorbed in nanoporous Si [19]. The combination of semiconductor and nanomagnet offers the

possibility of an integrated and scalable Q-bit system. The magnetization curves of this composite indicate that the $\{Cu_3\}$ rings enter into the nanopores, retaining their shapes. Results show that the spin–spin relaxation time is as long as 1.2 μs. The spin–lattice relaxation time is between 0.2-0.3 ms. A clear Rabi oscillation of nearly two cycles is observed between 1.5 K and 2 K. It is particularly interesting that the spin–spin relaxation time does not depend much on the doping of the Si. A further investigation of the interaction between the spin of $\{Cu_3\}$ and the conduction electron of Si is necessary for this point.

6. Portable pulsed magnet for tabletop spectrometer

A pulsed magnet is used to generate high magnetic fields, which cannot be obtained by superconducting and resistive magnets. Data acquisition demands a special technique because of the time dependence of the magnetic field. Advantages of a pulse magnet are the design diversity and the possibility of various custom applications. Recently, a concept of "portable magnet" has been developed to perform X-ray and neutron experiments in high magnetic fields [20-22].
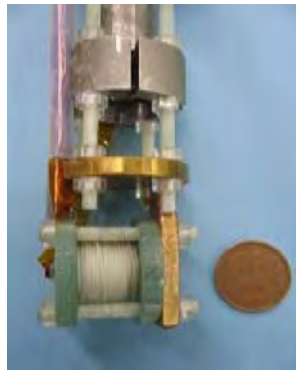
Fig. 7 Portable magnet used for the X-ray spectroscopy.

The energy needed for a pulse magnet is well known to scale with the product of volume and magnetic field intensity. When a magnet is downsized, the energy can be reduced and the power supply can be compact. Another advantage of a small magnet is the reduction of the stress of the magnet. The stress on the magnet wire is linear to the diameter and so the reduction of the magnet bore contributes to the decrease of magnet stress. In fact, a pulse magnet of 3 mm inner diameter generating 50 T is used for X-ray spectroscopy. The magnet is portrayed in Fig. 7. The portable magnet system is used for neutron diffraction in different facilities.

A similar system can be combined with a THz time domain spectrometer. For compactness of the magnet, the system can be put easily on the optical bench of the spectrometer. The use of the direct optics is easy in this case, which widens the THz wave bandwidth. The THz TDS in pulsed magnetic field can be a new type of ESR with white THz radiation. As such, application of a portable pulsed magnet will contribute to the development of THz ESR in a high magnetic field.

7. Summary

In summary, THz ESR can provide a unique and a powerful tool to investigate nanomagnets. It

is necessary to characterize nanomagnets to capture the short-range correlation and to manipulate the spin Q-bit. The range of application will be extended by the development of a tabletop pulsed magnet.

Acknowledgement

References

[1] H. Nojiri, Y. Ajiro, T. Asano et al. "Magnetic excitation of S=1/2 antiferromagnetic spin chain Cu benzoate in high magnetic fields", *New J. Phys.,* 8, 218, (2006).

[2] S. L. Wang, L. Li, Z. W. Ouyang et al. "Development of pulsed high magnetic field high frequency ESR facility", *Acta Physica Sinica*, in press (in Chinese)

[3] R. Watanabe, K. Fujiwara, A. Okazawa et al. "Chemical Trend of Ln-M Exchange Couplings in Heterometallic Complexes with Ln = Gd, Tb, Dy, Ho, Er and M = Cu, V", *Chem. Commun.*, 47, 2110–2112, (2011).

[4] F. Mori, T. Nyui, T. Ishida et al. "Oximate-bridged Trinuclear Dy–Cu–Dy Complex Behaving as a Single-molecule Magnet and Its Mechanistic Investigation", *J. Am. Chem. Soc.,* 128, 1440–1441, (2006).

[5] S. Ueki, A. Okazawa, T. Ishida et al. "Tetranuclear heterometallic cycle Dy_2Cu_2 and the corresponding polymer showing slow relaxation of magnetization reorientation", *Polyhedron*, 26, 1970–1676, (2007).

[6] A. Okazawa, T. Nogami, H. Nojiri et al. "Exchange Coupling and Energy-Level Crossing in a Magnetic Chain $[Dy_2Cu_2]_n$ Evaluated by High-Frequency Electron Paramagnetic Resonance", *Chem. Mater.,* 20, 3110–3119, (2008).

[7] A. Okazawa, T. Nogami, H. Nojiri et al. "Ferromagnetic Dy–Ni and Antiferromagnetic Dy–Cu Couplings in Single-Molecule Magnets [Dy₂Ni] and [Dy₂Cu]", *Inorg. Chem.,* 47, 9763–9765, (2008).

[8] Y. Oshima, H. Nojiri, J. Schnack et al. "Determination of Exchange Energies in the Sawtooth Spin Ring $\{Mo_{75}V_{20}\}$ by ESR", *Phys. Rev. B*, 85, 024413, (2012).

[9] A. Müller, M. Luban, C. Schröder et al. "Classical and Quantum Magnetism in Giant Keplerate Magnetic Molecules", *ChemPhysChem*, 2, 517, (2001).

[10] O. Cépas and T. Ziman, "Modified Spin-Wave Theory for Nanomagnets: Application to the Keplerate Molecule $\{Mo_{72}Fe_{30}\}$", *Prog. Theor. Phys. Suppl.,* 159, 280, (2005).

[11] M. Hasegawa and H. Shiba, "Magnetic Frustration and Anisotropy Effects in Giant Magnetic Molecule $Mo_{72}Fe_{30}$", *J. Phys. Soc. Jpn.,* 73, 2543–2549, (2004).

[12] C. Schröder, H. Nojiri, J. Schnack et al. "Competing Spin Phases in Geometrically Frustrated Magnetic Molecules", *Phys. Rev. Lett.,* 94, 017205, (2005).

[13] A. Ardavan, O. Rival, J. J. L. Morton et al. "Will Spin-Relaxation Times in Molecular Magnets Permit Quantum Information Processing?", *Phys. Rev. Lett.,* 98, 057201, (2007).

[14] A. M. Tyryshkin, S. A. Lyon, A. V. Astashkin et al. "Electron spin relaxation times of phosphorus donors in silicon", *Phys. Rev. B*, 68, 193207, (2003).

[15] G. Mitrikas, Y. Sanakis, C. P. Raptopoulou et al. "Electron spin–lattice and spin–spin relaxation study of a trinuclear iron(III) complex and its relevance in quantum computing", *Phys. Chem. Chem. Phys.,* 10, 743–748, (2008).

[16] S. Bertaina, S. Gambarelli, T. Mitra et al. "Quantum oscillations in a molecular magnet", *Nature*, 453, 203, (2008).

[17] C. Schlegel, J. van Slageren, M. Manoli et al. "Direct Observation of Quantum Coherence in Single-Molecule Magnets", *Phys. Rev. Lett.,* 101, 147203, (2008).

[18] S. Takahashi, J. van Tol, C. C. Beedle et al. "Coherent Manipulation and Decoherence of S=10 Single-Molecule Magnets", *Phys. Rev. Lett.,* 102, 087603, (2009).

[19] K.-Y. Choi, Z. X. Wang, H. Nojiri et al. "Coherent Manipulation of Electron Spins in the {Cu_3} Spin Triangle Complex Impregnated in Nanoporous Silicon", *Phys. Rev. Lett.,* 108, 067206, (2012).

[20] Y. H. Matsuda, T. Inami, K. Ohwada et al. "High-magnetic-field x-ray absorption spectroscopy of field-induced valence transition in $YbInCu_4$", *J. Phys. Soc. Jpn.,* 76, 034702, (2007).

[21] Y. H. Matsuda, Z.W. Ouyang, H. Nojiri et al. "X-Ray Magnetic Circular Dichroism of a Valence Fluctuating State in Eu at High Magnetic Fields", *Phys. Rev. Lett.,* 103, 046402, (2009).

[22] S. Yoshii, K. Ohoyama, K. Kurosawa et al. "Neutron Diffraction study on the Multiple Magnetization Plateaus in TbB_4 under Pulsed High Magnetic Field", *Phys. Rev. Lett.,* 103, 077203, (2009).